Criegee Intermediates Hot Paper

Deutsche Ausgabe: DOI: 10.1002/ange.201509685
Internationale Ausgabe: DOI: 10.1002/anie.201509685

The Origin of the Reactivity of the Criegee Intermediate: Implications for Atmospheric Particle Growth

*Evangelos Miliordos and Sotiris S. Xantheas**

Abstract: *The electronic structure of the simplest Criegee intermediate, H_2COO, is practically that of a closed shell. On the biradical scale (β), where 0 corresponds to the pure closed shell and 1 to a pure biradical, its β value is only 0.10, suggesting that its ground electronic state is best described as a $H_2C{=}O^{\delta+}{-}O^{\delta-}$ zwitterion. However, this picture of a nearly inert closed shell contradicts its rich reactivity in the atmosphere. It is shown that the mixing of its ground state with the first triplet excited state, which is a pure biradical state of the type $H_2C^{\bullet}{-}O{-}O^{\bullet}$, is responsible for the formation of strongly bound products during reactions inducing atmospheric particle growth.*

The role of Criegee intermediates (carbonyl oxides) in the chemical processes that occur in the troposphere has recently received a lot of attention[1–10] as their role in atmospheric particle formation has been recognized.[11–14] Taatjes and co-workers produced the Criegee intermediate through the reaction of CH_2I with O_2.[1] They recorded its photoionization mass spectrum and studied its reaction kinetics with NO, H_2O, SO_2, and NO_2. Using the same reaction to produce H_2COO, Lester and co-workers reported its ultraviolet spectrum; the absorption at 320–350 nm was attributed to the $B^1A'\rightarrow X^1A'$ electronic excitation and leads to photodissociation.[10] More recently, its infrared absorption spectrum,[15] self-interaction mechanisms,[13] and its reaction with water vapor[9] have been described. These intermediates are produced when unsaturated hydrocarbons react with ozone (ozonolysis),[16] and their immediate environment determines their fate. For this reason, their reactions with atmospherically abundant species, such as H_2O, NO, SO_2, and RO_2, have also been considered.[11,17–20] Note that the smallest member of this series, H_2COO, is isoelectronic to O_3 and can participate in ozonolysis-type reactions.[21,22]

Owing to its significance, the H_2COO intermediate has been the subject of numerous experimental[1–10,15,23–31] and theoretical[23,32–39] studies. Although early theoretical work indicated that H_2COO is of biradical nature, $H_2C^{\bullet}{-}O{-}O^{\bullet}$,[40,41] this view has changed over the years. Indeed, two recent reports have clearly demonstrated that H_2COO is better described as the $H_2C{=}O^{\delta+}{-}O^{\delta-}$ zwitterion, both from the theoretical[42,43] and experimental viewpoints.[15] Our own analysis[43] suggested that a value as small as 0.10 should be assigned to its biradical character (β), where a value of $\beta=0$ corresponds to a purely closed-shell molecule and $\beta=1$ to a genuine biradical. It is noteworthy that the first multi-configuration calculations, which were reported by Karlström et al. in 1979 and certainly are of limited accuracy compared to current computational capabilities, suggested two different optimum geometries for the ground state of H_2COO.[44]

However, the notion of a seemingly inert closed-shell molecule (consistent with a small value of β) contradicts its observed rich reactivity in the atmosphere. The H_2COO intermediate forms bound complexes when interacting not only with radical systems such as $NO^{\bullet}$ or $CH_3COO^{\bullet}$,[11] but also with closed-shell molecules such as H_2O,[17] SO_2,[11] $H_2C{=}CH_2$,[21] O_3,[45] and other organic compounds.[2,4] Its reaction with alkyl radicals is one of the key steps in atmospheric particle formation.[11]

To understand this apparent inconsistency between its theoretically predicted electronic structure and the observed behavior, we focused on the electronic manifold and in particular on its first few excited electronic states with the intent to investigate how they influence its atmospheric reactivity and especially the particle formation process. Surprisingly, we are aware of just two recent theoretical studies that deal with the excited states of this species, and only one of them considered the optically accessible excited states of singlet spin multiplicity. Aplincourt et al.[32] reported vertical excitation energies for the four singlet states (two of $^1A'$ and two of $^1A''$ symmetry) and predicted that the photochemical reactivity of H_2COO in the troposphere is associated with the aforementioned transitions, something that was subsequently experimentally confirmed by Lester and co-workers.[10] Lee et al.[23] examined the same vertical excitations aside from the $B^1A'\rightarrow X^1A'$ adiabatic one by applying about 30 different electronic-structure theory levels, including density functional, complete active space self-consistent field, coupled cluster, and configuration interaction calculations with different basis sets. A recent detailed analysis of the ground-state wavefunctions for the isomers of H_2COO revealed quite complex electronic-structure patterns, especially around the transition states of their interconversion pathways.[34]

The geometries, electronic configurations, as well as both the vertical and adiabatic excitation energies for the first five electronic states of H_2COO under C_s symmetry, namely X^1A', a^3A', b^3A'', A^1A'', and B^1A', are listed in Table 1. Our MCSCF/cc-pVTZ bond lengths and angles are within <0.02 Å and $<1°$ from the recently reported CCSD(T)-F12/aug-cc-pV5Z values.[30] Based on the MCSCF electronic

[*] Dr. E. Miliordos, Dr. S. S. Xantheas
Physical Sciences Division
Pacific Northwest National Laboratory
902 Battelle Boulevard, P.O. Box 999, MS K1-83, Richland, WA 99352 (USA)
E-mail: sotiris.xantheas@pnnl.gov
ORCID(s) from the author(s) for this article is/are available on the WWW under http://dx.doi.org/10.1002/anie.201509685

Table 1: Geometric parameters, adiabatic and vertical excitation energies, and Lewis structures for the first five electronic states of H_2COO with C_s symmetry at the MCSCF/cc-pVTZ level of theory.

	X^1A'	a^3A'	b^3A''	A^1A''	B^1A'
R(O–O) [Å]	1.351	1.360	1.418	1.437	1.764
R(C–O) [Å]	1.285	1.421	1.390	1.386	1.351
φ(O-O-C) [°]	118.2	108.0	107.9	107.2	100.3
R(C–H_a)[a] [Å]	1.070	1.064	1.064	1.064	1.063
R(C–H_b)[a] [Å]	1.069	1.066	1.064	1.064	1.070
φ(O-C-H_a)[a] [°]	119.4	117.7	120.0	120.2	120.6
φ(O-C-H_b)[a] [°]	114.7	113.8	112.7	112.6	113.7
T_e (adiabatic) [eV]	0.00	1.40	1.94	2.00	2.87
T_e (vertical) [eV]	0.00	1.87	2.27	2.37	4.42
Electronic structure					mixture[b]

[a] H_a is found towards the terminal O side, whereas H_b resides at the opposite side. [b] The B^1A' state has a composite wavefunction, see text.

configurations and the corresponding natural orbitals, we composed the simple Lewis diagrams shown in Table 1 that best describe these states. The carbon and the central oxygen atoms are connected by a double bond in the ground state X^1A' as opposed to the single C–O bond present in the next three states. This picture is consistent with the corresponding CO bond lengths. The values of R(CO) for the first three excited states of Table 1 are in the range of 1.40 ± 0.02 Å, whereas the bond length for the ground state is 1.285 Å and thus approximately 0.1 Å shorter. The bonding in the B^1A' state is less clear. The wavefunction for that state is a mixture of the ground state, the open singlet counterpart of the a^3A' state, and additional components that are less important. The R(OO) bond length of this state is much longer than that of any other state. As a result, its vertical and adiabatic excitation energies differ by as much as 1.55 eV, whereas this difference is < 0.5 eV for the other four states. The geometries of the $^{1,3}A''$ states are very similar to each other as expected from the fact that they are associated with identical Lewis diagrams describing their electronic structure. The ground-state geometry of Table 1 is the global minimum with the nine harmonic frequencies being 540, 653, 849, 881, 1245, 1294, 1581, 3300, and 3460 cm^{-1}. However, the planar geometry of the first triplet state is a first-order transition state. An unconstrained geometry optimization yielded a structure with the two hydrogen atoms being out of the plane in the same direction, with the two dihedral angles being $\theta_a(H_aCOO) = 47.6°$ and $\theta_b(H_bCOO) = 32.8°$ and the rest of the geometrical parameters practically unchanged from the ones of the planar transition state. The B^1A' state had experimentally been found to be dissociative.[12]

If the ground state of H_2COO were a true biradical, in which case an electron would be localized on the carbon atom, the formation of a covalent bond between that lone electron and an approaching H atom would be spontaneous. The full potential energy curves (PECs) for the first three electronic states describing the approach of H to H_2COO are shown in Figure 1 with respect to the distance between the two reactants. The rest of the geometrical parameters were fully optimized for the ground-state PECs, and these values were used for the calculation of the two excited-state PECs. It was found that only the C–O bond length of the H_2COO moiety changes appreciably during the H+H_2COO approach. Figure 2 shows the optimal H_2C–OO and H_2CO–O lengths with respect to the H–CH_2OO distance along the PEC.

The ground-state adiabatic fragments at large separations are H_2COO (X^1A') and H (^2S). As already mentioned earlier, the ground state of H_2COO is rather a closed shell, and thus the PEC correlating with the lowest-energy fragments ($^2A'$) is expected to be

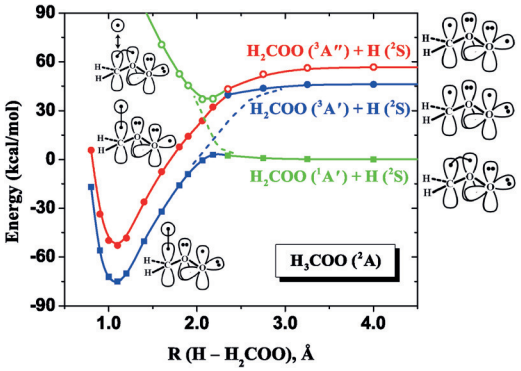

Figure 1. Potential energy curves describing the H–H_2COO interaction. The ground-state complex (blue curve) clearly originates from the first triplet excited state of the Criegee intermediate. The Lewis structures of the various stable complexes as well those of their asymptotic products are shown.

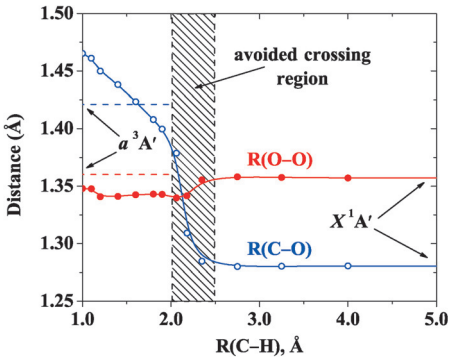

Figure 2. Optimal H_2CO–O (red) and H_2C–OO (blue) bond lengths as a function of the H–CH_2OO distance for the ground-state potential energy curve in Figure 1.

repulsive (green line in Figure 1). The first excited dissociation channel, H_2COO ($^3A'$)+H (^2S), shown in blue in Figure 1, correlates with a state of the same symmetry ($^2A'$) and a more conventional binding motif: One of the two lone electrons of

the triplet state of H_2COO couples with the single electron of H to form a covalent bond, whereas the other one remains practically unaffected (i.e., it is an observer). The same is true for the next dissociation channel, H_2COO ($^3A''$)+H (^2S), shown in red in Figure 1, but now the observer electron occupies a different orbital (see the valence-bond Lewis structures in Figure 1). These results suggest that there are two attractive PECs emanating from the first two excited adiabatic channels, whereas the one correlating with the ground-state fragments is repulsive. Their "mixing" results in the final picture that is shown in Figure 1. The lowest PEC of Figure 1 describes a binding interaction for distances shorter than approximately 2.0 Å owing to the mixing with the first excited adiabatic channel. The repulsive character of the ground state is conveyed to the next two PECs, which cross at approximately the same distance. The question of whether this is a real or an avoided crossing involves the consideration of a multidimensional potential energy surface and is beyond the purpose of the present study.

An additional indication of the strong interaction of the two lowest PECs is the sudden elongation of the C–O bond for H–CH_2OO distances between 2.0 and 2.5 Å (avoided crossing region). In this region, the C–O bond length increases from 1.285 Å (equilibrium value for the X^1A' state of H_2COO) to 1.375 Å at R(H–C) = 2.0 Å and to even larger values for shorter H–CH_2OO distances. The equilibrium C–O length of the a^3A' excited state of H_2COO is 1.421 Å (see Table 1). This observation further supports the gradual exchange in the electronic structure between the two PECs. The H_2C–O–O skeleton is practically unaffected during the reaction whereas the change in R(C–O), which is due to the mixing of the electronic states, occurs in the avoided crossing region; this is consistent with the complex wavefunction structure reported by Kalinowski et al.[34] for the "off-equilibrium" geometries. At equilibrium, we have two distinct electronic doublet states (X^2A'', A^2A') within approximately 20 kcal mol^{-1} that can be distinguished by the fact that the lone electron resides in different orbitals that are localized mostly on the end oxygen atom, reflecting the electronic structure of the first two excited (triplet) states of H_2COO (see also the Lewis diagrams in Figure 1). In simple terms, the Criegee intermediate at its equilibrium geometry is mainly a closed shell ($\beta = 0.1$) but when the H atom approaches, its incipient electronic structure changes and adopts the character of the first excited state (which is a biradical), a fact that is consistent with the corresponding changes in the geometry in the region where the two states mix. A more pedagogical example would be the fact that the electronic state of carbon in methane is not that of the atom's ground state but rather that of its ^5S excited states, a change that is facilitated by its interaction with the H atoms.[46,47]

The product of the model reaction described in Figure 1 is the H_3COO radical with a lone electron localized on the endmost oxygen atom. This molecule has been considered as the initiator for the polymerization of H_2COO. First H_3COO binds to a H_2COO molecule, producing a new radical ($H_3COOCH_2COO^{\bullet}$), which in turn reacts with another H_2COO molecule and so forth.[11] For this reason, we investigated the first step in the above polymerization

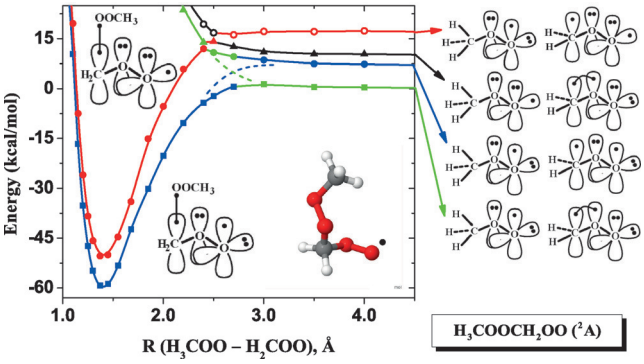

Figure 3. PECs for the H_3COO–CH_2OO interaction. The ground-state complex (blue) clearly originates from the first triplet excited state of the Criegee intermediate (red). The Lewis structures of the various stable complexes as well those of their asymptotic products are shown.

reaction, namely the approach of a H_3COO radical to a Criegee H_2COO intermediate. Four PECs, which are shown in Figure 3, were constructed to describe the H_3COO–H_2COO interaction. These PECs were constructed by varying the distance between the terminal O atom of H_3COO and the C atom of H_2COO. We kept all internal coordinates of the two fragments fixed at their ground-state equilibrium values, while we optimized their relative orientation (five angles). The geometries used for the excited PECs are those of the ground-state PEC. More accurate geometries of the stationary points of the ground-state PEC can be found in Ref. [11]. According to our previous discussion, the first two states of H_3COO have one lone electron localized on the terminal oxygen atom. In the ground state, this electron is "perpendicular" to the COO plane, whereas it lies in that plane in the first excited state. Combining the states of the H_3COO and H_2COO fragments, the first four adiabatic channels correspond to H_3COO (X^2A'')+H_2COO (X^1A'), H_3COO (X^2A'')+H_2COO (a^3A'), H_3COO (A^2A')+H_2COO (X^1A'), and H_3COO (X^2A'')+H_2COO (b^3A''). As in the case of the H–H_2COO interaction, we have a system with one lone electron approaching the Criegee intermediate, but now the steric repulsion is also a factor. Overall, we have the same scenario as that shown in Figure 1. The fragments based on the practically closed-shell ground state of H_2COO are expected to yield a repulsive PEC, and the triplet states of H_2COO are expected to produce strongly bound PECs. Indeed, this is the case, with the red and blue PECs in Figure 3 being attractive and strongly interacting whereas the black and green PECs are originally dissociative. The interaction between all of these PECs yields the adiabatic ones shown in Figure 3. In both Figure 1 and Figure 3, the two bound PECs (shown in blue and red) are parallel to each other for short distances (≤ 2 Å), a fact that suggests a similarity in their bonding mechanism. Furthermore, the equilibrium structure of the first excited state (red curve) asymptotically correlates with the fragments that are highest in energy among the four considered here, and it is stabilized by complex interactions between the PECs that occur at approximately 2.4 Å.

In conclusion, we have studied the interaction of the smallest member of the Criegee intermediates, H_2COO, with

radical systems. Our analysis is consistent with the hypothesis that the H_2COO intermediate is indeed a closed-shell system, with its ground-state minimum geometry best represented as the $H_2C{=}O^{\delta+}{-}O^{\delta-}$ zwitterion. However, its first triplet excited state, which is a pure biradical with the Lewis structure $H_2C^{\bullet}{-}O{-}O^{\bullet}$, is responsible for its reactions. The current results can be generalized for larger Criegee intermediates by replacing the terminal H atoms with larger organic chains.[3]

Experimental Section

We employed the multiconfiguration self-consistent field (MCSCF) method. For the approach of H to H_2COO, the active space consisted of 19 electrons and 13 orbitals, yielding 104104 configuration state functions (CSFs). The two C–H "antibonding" molecular orbitals were excluded from the complete active space of 15 orbitals; these two orbitals were not considered to be essential because none of the C–H bonds were broken in the process. The same active space, but without the 1s orbital of hydrogen, was used for the isolated H_2COO molecule. For the H_3COO–H_2COO interaction, we used an active space of 7 electrons and 5 orbitals (40 CSFs), which are needed for describing the first four doublet electronic states. We used the triple-ζ quality correlation consistent basis set (cc-pVTZ) of Dunning and coworkers,[48] consisting of the segmented contractions of 3s2p1d basis functions for H and 4s3p2d1f for C and O.

Acknowledgements

This work was supported by the US Department of Energy, Office of Science, Office of Basic Energy Sciences, Division of Chemical Sciences, Geosciences & Biosciences at Pacific Northwest National Laboratory (PNNL), a multi-program national laboratory operated for the DOE by Battelle. This research used resources of the National Energy Research Scientific Computing Center, which is supported by the Office of Science of the U.S. Department of Energy (DE-AC02-05CH11231).

Keywords: atmospheric chemistry · biradicals · computational chemistry · Criegee intermediates · electronic structure

How to cite: *Angew. Chem. Int. Ed.* **2016**, *55*, 1015–1019
Angew. Chem. **2016**, *128*, 1027–1031

[1] O. Welz, J. D. Savee, D. L. Osborn, S. S. Vasu, C. J. Percival, D. E. Shallcross, C. A. Taatjes, *Science* **2012**, *335*, 204–207.
[2] C. A. Taatjes, O. Welz, A. J. Eskola, J. D. Savee, D. L. Osborn, E. P. F. Lee, J. M. Dyke, D. W. K. Mok, D. E. Shallcross, C. J. Percival, *Phys. Chem. Chem. Phys.* **2012**, *14*, 10391–10400.
[3] C. A. Taatjes, O. Welz, A. J. Eskola, J. D. Savee, A. M. Scheer, D. E. Shallcross, B. Rotavera, E. P. F. Lee, J. M. Dyke, D. K. W. Mok, D. L. Osborn, C. J. Percival, *Science* **2013**, *340*, 177–180.
[4] L. Vereecken, *Science* **2013**, *340*, 154–155.
[5] P. Aplincourt, M. F. Ruiz-López, *J. Phys. Chem. A* **2000**, *104*, 380–388.
[6] R. M. Harrison, J. Yin, R. M. Tilling, X. Cai, P. W. Seakins, J. R. Hopkins, D. L. Lansley, A. C. Lewis, M. C. Hunter, D. E. Heard, L. J. Carpenter, D. J. Creasy, J. D. Lee, M. J. Pilling, N. Carslaw, K. M. Emmerson, A. Redington, R. G. Derwent, D. Ryall, G. Mills, S. A. Penkett, *Sci. Total Environ.* **2006**, *360*, 5–25.
[7] D. Johnson, G. Marston, *Chem. Soc. Rev.* **2008**, *37*, 699–716.
[8] L. Vereecken, J. S. Francisco, *Chem. Soc. Rev.* **2012**, *41*, 6259–6293.
[9] W. Chao, J.-T. Hsieh, C.-H. Chang, J. J.-M. Lin, *Science* **2015**, *347*, 751.
[10] J. M. Beames, F. Liu, L. Lu, M. I. Lester, *J. Am. Chem. Soc.* **2012**, *134*, 20045–20048.
[11] L. Vereecken, H. Harder, A. Novelli, *Phys. Chem. Chem. Phys.* **2012**, *14*, 14682–14695.
[12] M. C. McCarthy, L. Cheng, K. N. Crabtree, O. Martinez, Jr., T. L. Nguyen, C. C. Womack, J. F. Stanton, *J. Phys. Chem. Lett.* **2013**, *4*, 4133–4139.
[13] Y.-T. Su, H.-Y. Lin, R. Putikam, H. Matsui, M. C. Lin, Y.-P. Lee, *Nat. Chem.* **2014**, *6*, 477.
[14] C. A. Taatjes, D. E. Shallcross, C. J. Percival, *Phys. Chem. Chem. Phys.* **2014**, *16*, 1704.
[15] Y. T. Su, Y. H. Huang, H. A. Witek, Y. P. Lee, *Science* **2013**, *340*, 174–176.
[16] R. Criegee, *Angew. Chem. Int. Ed. Engl.* **1975**, *14*, 745; *Angew. Chem.* **1975**, *87*, 765.
[17] J. M. Anglada, J. González, M. Torrent-Sucarrat, *Phys. Chem. Chem. Phys.* **2011**, *13*, 13034–13045.
[18] L. Jiang, R. Lan, Y. S. Xu, W. J. Zhang, W. Yang, *Int. J. Mol. Sci.* **2013**, *14*, 5784–5805.
[19] B. Long, X. F. Tan, Z. W. Long, Y. B. Wang, D. S. Ren, W. J. Zhang, *J. Phys. Chem. A* **2011**, *115*, 6559–6567.
[20] M. Nakajima, Y. Endo, *J. Chem. Phys.* **2014**, *140*, 034318.
[21] R. Crehuet, J. M. Anglada, D. Cremer, J. M. Bofill, *J. Phys. Chem. A* **2002**, *106*, 3917–3929.
[22] Z. J. Buras, R. M. I. Elsamra, A. Jalan, J. E. Middaugh, W. H. Green, *J. Phys. Chem. A* **2014**, *118*, 1997–2006.
[23] E. P. F. Lee, D. K. W. Mok, D. E. Shallcross, C. J. Percival, D. L. Osborn, C. A. Taatjes, J. M. Dyke, *Chem. Eur. J.* **2012**, *18*, 12411–12423.
[24] Z. J. Buras, R. M. I. Elsamra, W. H. Green, *J. Phys. Chem. Lett.* **2014**, *5*, 2224–2228.
[25] Y. Liu, K. D. Bayes, S. P. Sander, *J. Phys. Chem. A* **2014**, *118*, 741–747.
[26] L. Lu, J. M. Beames, M. I. Lester, *Chem. Phys. Lett.* **2014**, *598*, 23–27.
[27] W.-L. Ting, Y.-H. Chen, W. Chao, M. C. Smith, J. J.-M. Lin, *Phys. Chem. Chem. Phys.* **2014**, *16*, 10438–10443.
[28] L. Sheps, *J. Phys. Chem. Lett.* **2013**, *4*, 4201–4205.
[29] J. H. Lehman, H. Li, J. M. Beames, M. I. Lester, *J. Chem. Phys.* **2013**, *139*, 141103.
[30] M. Nakajima, Y. Endo, *J. Chem. Phys.* **2013**, *139*, 244310.
[31] A. M. Daly, B. J. Drouin, S. Yu, *J. Mol. Spectrosc.* **2014**, *297*, 16–20.
[32] P. Aplincourt, E. Henon, F. Bohr, M. F. Ruiz-Lopez, *Chem. Phys.* **2002**, *285*, 221–231.
[33] M. T. Nguyen, T. L. Nguyen, V. T. Ngan, H. M. T. Nguyen, *Chem. Phys. Lett.* **2007**, *448*, 183–188.
[34] J. Kalinowski, M. Rasanen, P. Heinonen, I. Kilpelainen, R. B. Gerber, *Angew. Chem. Int. Ed.* **2014**, *53*, 265–268; *Angew. Chem.* **2014**, *126*, 269–272.
[35] A. Karton, M. Kettner, D. A. Wild, *Chem. Phys. Lett.* **2013**, *585*, 15–20.
[36] J. Li, S. Carter, J. M. Bowman, R. Dawes, D. Xie, H. Guo, *J. Phys. Chem. Lett.* **2014**, *5*, 2364–2369.
[37] K. Samanta, J. M. Beames, M. I. Lester, J. E. Subotnik, *J. Chem. Phys.* **2014**, *141*, 134303.
[38] W.-m. Wei, R.-h. Zheng, Y.-l. Pan, Y.-k. Wu, F. Yang, S. Hong, *J. Phys. Chem. A* **2014**, *118*, 1644–1650.
[39] M. Nakajima, Y. Endo, *J. Chem. Phys.* **2014**, *140*, 034318.
[40] L. B. Harding, W. A. Goddard III, *J. Am. Chem. Soc.* **1978**, *100*, 7180–7188.

[41] W. Sander, *Angew. Chem. Int. Ed. Engl.* **1990**, *29*, 344 – 354; *Angew. Chem.* **1990**, *102*, 362 – 372.
[42] D. Cremer, J. Gauss, E. Kraka, J. F. Stanton, R. J. Bartlett, *Chem. Phys. Lett.* **1993**, *209*, 547 – 556.
[43] E. Miliordos, K. Ruedenberg, S. S. Xantheas, *Angew. Chem. Int. Ed.* **2013**, *52*, 5736 – 5739; *Angew. Chem.* **2013**, *125*, 5848 – 5851.
[44] G. Karlström, S. Engström, B. Jönsson, *Chem. Phys. Lett.* **1979**, *67*, 343 – 347.
[45] H. G. Kjaergaard, T. Kurtén, L. B. Nielsen, S. Jørgensen, P. O. Wennberg, *J. Phys. Chem. Lett.* **2013**, *4*, 2525 – 2529.
[46] A. Papakondylis, E. Miliordos, A. Mavridis, *J. Phys. Chem. A* **2004**, *108*, 4335 – 4330.
[47] A. Kalemos, T. H. Dunning, Jr., A. Mavridis, J. F. Harrison, *Can. J. Chem.* **2004**, *82*, 684 – 693.
[48] T. H. Dunning, Jr., *J. Chem. Phys.* **1989**, *90*, 1007 – 1023.

Received: October 15, 2015
Published online: December 7, 2015

